Journal of Innovative Image Processing (ISSN: 2582-4252)
www.irojournals.com/iroiip/

Explainable Artificial Intelligence with Deep Representation Learning Model for Polycystic Ovary Syndrome Detection Using Clinical Features

Veena Rani[1], Chandrasekar Venkatachalam[2], Karthick Raghunath K M.[3]

[1]Research Scholar, Department of Computer Science and Engineering, JAIN (Deemed - to - be University), Kanakapura Campus, Bangalore, Karnataka, India.
[2]Professor, [3]Associate Professor, Department of Computer Science and Engineering, Faculty of Engineering and Technology, JAIN (Deemed - to - be University), Kanakapura Campus, Bangalore, Karnataka, India.

E-mail: [1]v4veena.rani@gmail.com, [2]chandrasekar.v@jainuniversity.ac.in, [3]karthick.km@jainuniversity.ac.in

Orcid ID: [1]0009-0004-0456-9517, [2]0000-0001-7258-0794, [3]0000-0002-6948-5240

Abstract

Polycystic Ovary Syndrome (PCOS) is a prevalent endocrine condition affecting females and requires timely diagnosis for appropriate management and to mitigate long-term adverse problems. It is a complex condition identified by medical features such as hormonal imbalance, the existence of numerous ovarian follicles, irregular menstrual cycles, and anovulation. Over the past few years, Artificial Intelligence and deep learning approaches have demonstrated positive outcomes in medical applications by allowing effective analysis of intricate medical data. This study introduces an Explainable Artificial Intelligence-based Deep Representation Learning Model for Polycystic Ovary Syndrome Detection (XAIDRL-PCOSD). The proposed approach aims to support early and reliable detection of PCOS by leveraging real-world patient data. The model applies a hybrid feature selection strategy combining mutual information, recursive feature elimination, and LASSO to recognize the most significant clinical attributes. For classification, a feature tokenization transformer is employed to learn deep feature representations and capture complex relationships among clinical parameters. During training, the Ranger optimizer is utilized to enhance convergence and overall model performance. In addition, explainable artificial intelligence is incorporated using SHAP to provide clear insights into feature contributions, enhancing the interpretability of the model's predictions for both PCOS and No PCOS cases. The experimental outcomes show that the proposed model accomplishes effective performance in PCOS detection with an accuracy of 95.71% while also offering transparency in decision-making. Therefore, the proposed XAIDRL-PCOSD model can serve as an effective tool in assisting medical professionals in understanding key factors influencing diagnosis.

Keywords: PCOS Detection, Deep Learning, FT-Transformer, Explainable Artificial Intelligence, Hybrid Feature Selection, Clinical Data.

DOI: https://doi.org/10.36548/jiip.2026.3.009
Received: 05.05.2026, received in revised form: 09.06.2026, accepted: 30.06.2026, published: 11.07.2026
© 2026 Inventive Research Organization. This is an open access article under the Creative Commons Attribution-NonCommercial International (CC BY-NC 4.0) License

1. Introduction

Polycystic Ovary Syndrome (PCOS) is a primary, prevalent factor leading to ovulatory infertility and is related to different health risks, including anovulation, ovarian cancer, and preterm abortions. This can impact almost 5% to 10% of women in their reproductive age [1]. Precisely diagnosing PCOS in professional medical practice constitutes a major challenge for radiologists because of the inconsistency in follicle sizes and their intricate relations with nearby tissues and blood vessels [2]. The medical signs of PCOS vary among individuals and may occur with no clear reasons. The medical analysis of PCOS depends on Rotterdam standards, which include polycystic ovaries, hyperandrogenism, and oligo-anovulation. Still, this disorder is a more complicated, diverse phenotype, impacted by genetics and intra- or extra-uterine pathophysiological-related disorders [3]. In order to manually detect PCOS, the medical experts and radiologists presently utilize ovarian ultrasonography to count the follicles and measure the volumes of both ovaries. Also, due to the health concerns of the patient, these medical experts should conduct further tests and medical analysis for biochemical and medical symptoms for the identification of PCOS [4].

The earlier identification of PCOS can support more effective control of physiological and emotional indications, possibly preventing major overall health problems. As reported by the WHO, up to 70% of PCOS patients are not diagnosed globally [5]. Thus, the criteria-based medical evaluation of PCOS presents a complexity to medical experts, a difficulty that is compounded by differences in the valuations of genetic aspects, menstrual irregularity, ecological influences, and oxidative stress. Automatic identification of PCOS in its preliminary phase depends on ultrasound (US) images and clinical data to support disease diagnosis. PCOS analysis has various approaches and diagnostic indicators that can be more essential for menstrual data, blood tests, and US analysis. Due to the variety of medical indications associated with this disorder and the nonappearance of a single analytical tool utilized by medical specialists for the evaluation of patients, medical experts are required to obtain the outcomes of laboratory analysis and redundant radiological images. Thus, PCOS is recognized by removing distinct medical indications or test outcomes because of the restricted data of its intricate pathomechanism [6]. At the same time, earlier diagnosis and identification of PCOS with reduced laboratory tests and imaging methods are crucial, as the above-mentioned disorder leads to ovarian dysfunction.

Innovative developments in machine learning (ML) and deep learning (DL) allow automatic PCOS identification through evaluating US and medical data, decreasing reliance on human management and helping medical decision-making [7]. ML and DL models have an outstanding performance in identification due to their ability to extract features. Hence, significant research has been performed for the identification of PCOS using ML and DL techniques. Consequently, this research is designed to offer additional foundations for the identification of PCOS and supplementary diagnostic approaches for the medical field, to increase the value of the application of these markers in the clinic, and to offer a different path for the ultimate diagnosis of the disease [8].

1.1 Problem Statement and Contributions of the Work

Even though a PCOS diagnosis comprises multiple clinical and biochemical factors, the overall process is still complex and often needs several tests and expert evaluation. As symptoms can vary from person to person and there is no single standard diagnostic technique, identifying PCOS at an early stage becomes difficult. Because of this, there is a need for a

system that can effectively examine clinical data more efficiently and assist in identifying PCOS in a simpler and more consistent way. With the increasing availability of healthcare data, advanced computational techniques can be utilized to support this process. DL models, especially those suitable for tabular data, can learn complex relationships between different clinical features and enhance prediction results. At the same time, it is also important to make these models understandable, so that the outcomes can be interpreted easily and trusted in real-world medical applications. Given this, the present work focuses on developing an effective and interpretable model for PCOS identification using clinical data. To accomplish this, this paper presents an Explainable Artificial Intelligence-based Deep Representation Learning Model (XAIDRL-PCOSD) for accurate detection of PCOS using clinical features. The overall framework includes data preprocessing to improve data quality, a hybrid feature selection strategy to identify important attributes, a DL-based classification model, model optimization, and XAI interpretation. The performance of the proposed approach is evaluated by employing various metrics. The major contributions of this manuscript are given below:

- Utilize a hybrid feature selection approach by incorporating mutual information (MI), recursive feature elimination (RFE), and LASSO to identify the most beneficial clinical features while removing unnecessary and redundant data, thereby improving model efficiency.
- Employ a deep learning model based on Feature Tokenizer-Transformer (FT-Transformer) for classification to learn the relationships between different clinical features and improve PCOS detection.
- Integrate the Ranger optimizer during training to stabilize the learning process and achieve better results.
- Apply SHAP as an explainability method to understand how different features affect the prediction.
- Conduct experiments on the PCOS dataset, examining model performance using measures like accuracy, precision, recall, F1-score, and MCC.

2. Related Work

In this section, a review of related works on PCOS detection and classification is presented, along with identified research gaps. Abed et al. [9] developed an innovative and robust technique to detect PCOS-related irregularities, such as cystic developments, thick ovarian tissues, and interrupted vascular patterns. Progressive image enhancement methods were utilized for preprocessing the data, while the Siamese Network investigated histological and structural features to detect the existence of PCOS. The above-mentioned method emphasizes the crucial role of ML methods, especially Siamese Networks, for medical diagnosis and imaging, thus enabling transparent and effective healthcare outcomes. Suvika et al. [10] addressed a significant gap in the research by methodically recognizing and removing noisy data during the pre-processing stage. This architecture highlighted the requirement for enhancing data processing to extend the perception of the intricate appearances and health consequences related to PCOS and PCOD. Ahmad et al. [11] presented three lightweight DL methods (CNN, LSTM, and CNN-LSTM), integrating SMOTE for dataset matching to acquire effective outcomes. Among all three methods, the SMOTE + CNN architecture performed with the highest outcomes with respect to classification measures. Furthermore, a performance

assessment was also executed with alternative recent PCOS identification research and techniques that can quantify higher system efficacy. Gollapalli et al. [12] developed a novel PCOS classification technique that combines the encoder part of a transformer module with different pretrained CNN architectures for robust feature extraction using US images. This approach aims to provide an extremely precise and wide-ranging PCOS detection method, thereby allowing earlier interventions and modified treatment plans.

Jain et al. [13] presented XAI to examine diverse aspects integrated into the disease, which ultimately assists in improved detection of PCOS. By examining data using XAI, it is noted that the most important element impacting PCOS is the insulin level. Thus, this study contributes to detecting the aspects accountable for PCOS utilizing XAI. Avasthi et al. [14] designed a novel model for early identification of PCOS using ML, particularly concentrating on the XGBoost model. By boosting timely identification abilities, this model greatly enhances patient outcomes and emphasizes the importance of data-based approaches in controlling PCOS. Nalawade et al. [15] aimed at training several pretrained approaches and a CNN, performing a comparative study on predictive precision. Moreover, XAI methods such as LIME are used to support healthcare staff in providing bias-free, accurate predictions promptly. Mondal et al. [16] presented a hybrid filter-wrapper technique for identifying the best features. Subsequently, a reinforcement learning-driven binary equilibrium optimizer is leveraged. In this study, RL utilized State-Action-Reward-State-Action (SARSA) for increasing the population variety in the search space to evade the issue of local optimum. Further, the identified optimum attributes are passed into the Bonferroni Mean Fuzzy KNN (BMFK) model for classification. Table 1 shows an overview of existing studies on PCOS detection.

Table 1. Overview of the related works on PCOS detection

Authors	Years	Objective	Method Used	Key Outcome
Abed et al. [9]	2026	To identify structural abnormalities in the ovaries for PCOS detection.	Siamese Network with image enhancement	Identified cysts, tissue variations, and vascular patterns effectively.
Suvika et al. [10]	2026	To remove noisy data and improve understanding of clinical patterns.	Optimized ML with PANN	Achieved better performance by capturing complex patterns in data.
Ahmad et al. [11]	2024	To improve prediction accuracy using a balanced dataset.	LSTM, CNN, CNN-LSTM with SMOTE	SMOTE + CNN achieved better accuracy, precision, recall, and AUC.
Gollapalli et al. [12]	2024	To enhance feature extraction from ultrasound images for PCOS detection.	Transformer encoder + pretrained CNN	Provided accurate and robust PCOS classification.
Jain et al. [13]	2024	To identify important clinical factors influencing PCOS.	Explainable AI (XAI)	Found insulin and follicle count as key features.
Avasthi et al. [14]	2024	To develop an accurate prediction model for PCOS detection.	XGBoost	Achieved high accuracy (around 96%).
Nalawade et al. [15]	2025	To improve prediction accuracy with explainability.	CNN + LIME	Achieved 99% accuracy with interpretable results.
Mondal et al. [16]	2025	To enable early detection with explainable predictions.	ANN + SHAP + SMOTETomek	Improved detection with better interpretability.

2.1 Research Gaps

Even though many studies have been done for PCOS detection using ML and DL methods, some issues are still present.

- In the work by Abed et al. [9], the focus is mainly on image-based detection using Siamese Networks. This model depends heavily on ultrasound images, so clinical data is not fully utilized, even though it can assist in early detection.
- Ahmad et al. [11] employed DL techniques with SMOTE for improving accuracy. The results are good, but the model does not clearly demonstrate how decisions are made, which can be a significant issue in medical applications.
- In another study, Jain et al. [13] used XAI to find important factors related to PCOS. It helps in understanding the features, but the model itself is not strong enough to learn more complex relationships between them.
- Avasthi et al. [14] used XGBoost and achieved good accuracy, but such models may miss some deeper patterns in clinical data.

From these examples, it can be understood that most works concentrate only on either performance or explainability. They are not combined properly to accomplish an interpretable and robust PCOS diagnostic performance. Because of this, there is a need for a model that can work well with clinical data, capture complex patterns, and also give understandable results. Therefore, the proposed model concentrates on the development of a DL-based PCOS detection model with enhanced interpretability, improved diagnostic accuracy, and reliable clinical decision-making.

3. Proposed Methodology

The proposed model follows a step-by-step approach for detecting PCOS using clinical data. The overall architecture of the XAIDRL-PCOSD approach is shown in Figure 1. The model mainly includes preprocessing, feature selection, classification, optimization, and explainability. First, the clinical dataset is pre-processed by handling missing values, removing outliers, and applying feature scaling so that the data becomes appropriate for analysis. After that, important features are chosen using a combination of MI, RFE, and LASSO, which helps in removing unnecessary features. Then, the selected attributes are provided to the FT-Transformer model for classification, where the model learns the relationships between different clinical parameters and predicts whether a case is PCOS or not. Moreover, the Ranger optimizer is utilized to enhance the learning process. Finally, SHAP is applied to understand how different features affect the prediction, which makes the model easier to interpret.

3.1 Data Pre-processing

Data preprocessing plays a main part in enhancing better results in the PCOS recognition method. In this phase, redundant and non-essential data are excluded from the PCOS dataset. Such data are irrelevant for model classification, and preprocessing supports increasing the efficiency of learning models. Besides improving accuracy, it also benefits from minimizing the time required for computation.

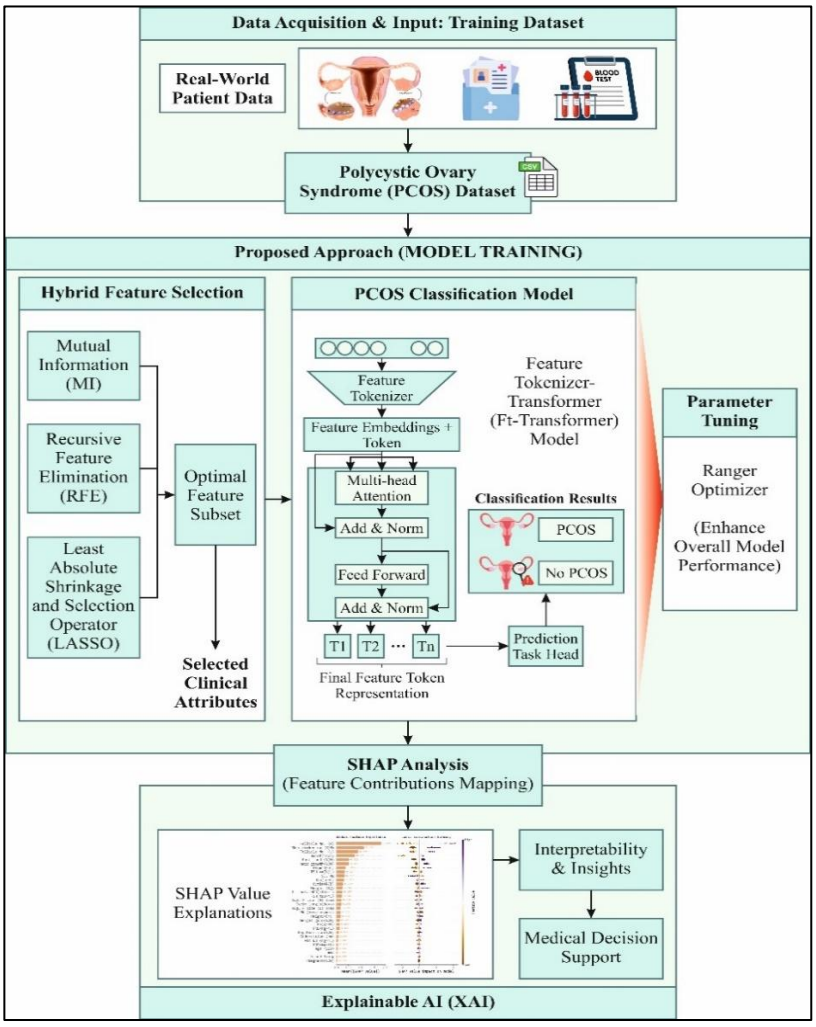

Figure 1. Overall architecture of the proposed XAIDRL-PCOSD methodology

Missing Value Handling: The KNN imputer is utilized to handle missing values in the dataset. In the current world, data are gathered from different origins and used for analytical purposes, generating insights, supporting theory validation, and various other applications. When data are collected from different sources, it often results in incomplete or missing details. Such issues can arise from errors during data extraction or collection, typically caused by humans. Hence, addressing missing data is an essential part of pre-processing. Selecting an appropriate imputation method is essential, as it significantly influences model performance. A widely adopted method for imputing missing entries is the KNN imputer performed on clinical features via scikit-learn. It is often utilized as a substitute for traditional imputation techniques. It can be represented as follows.

$$Dab = \sqrt{\frac{n}{m}} \sum_{i \in present} (ai - bi)^2 \quad (1)$$

In the above equation, the term D_{ab} represents the distance between samples a and b, m specifies the number of commonly observed (non-missing) features shared by both samples, n refers to the overall number of features, the notation $i \in present$ implies indices where both a_i and b_i are available, and it is the feature values of samples a and b.

Outlier Detection: Isolation Forest (IF) is utilized to detect and manage outliers. IF is a self-organizing ML method programmed to identify outliers by separating them rather than analyzing regular data patterns. By applying a random split on features, it detects outliers based on their shorter path lengths in trees due to their distinct nature. It labels them as -1 and inliers as 1, thereby improving the effectiveness of the PCOS classification model training. Here, the IF model is designed using 100 estimators with a contamination factor of 0.03 and a random state of 42. The algorithm labels anomalous instances as −1 and normal instances as +1 depending upon the average path length over isolation trees.

Feature Scaling: Employing feature scaling is essential to maintain consistency in the scale of all features. This ensures that each feature is equally weighted, which supports smoother processing by the model. This approach improves efficiency by recognizing anomalies related to their values instead of actual values. Using the StandardScaler to normalize clinical features, the features are adjusted to a single scale, which enhances the performance of the FT-Transformer method. The application of StandardScaler to each attribute X is defined mathematically:

$$X' = \frac{X - \gamma\iota}{\sigma} \tag{2}$$

Here X signifies the original value, X' denotes the standardized value, σ is the standard deviation value, and μ Stands for the mean value.

3.2 Hybrid Feature Selection Method

The presented method adopts a hybrid FS that integrates mutual information (MI), recursive feature elimination (RFE), and LASSO to select the most significant clinical features. By uniting these methods, the model retains features that are statistically significant and predictive, while filtering out less essential ones [17].

3.2.1 Mutual Information Algorithm

MI reduces the level of unpredictability of one variable when data from another variable is considered. MI evaluates the joint probability relationship of individual features along with the target ones. The MI for dual discrete random variables A and B can be given as follows,

$$I(A,B) = \sum_{a\in A}\sum_{b\in B} p\,(a,b)\log\left(\frac{p(a,b)}{p(a)p(b)}\right) \tag{3}$$

Here, the terms $p(a)$ and $p(b)$ correspond to their marginal distribution with respect to A and B, $p(a,b)$ denotes the joint distribution along with A and B. Upon handling continuous variables, the calculation of MI relies on density measurement using kernel or alternative numerical methods.

3.2.2 Recursive Feature Elimination

The RFE works in a retrogressive approach by eliminating features. This method starts by training all available features from the dataset, after which it assesses the relevance of all features depending on the evaluation metrics. It removes the less important feature while retaining the most relevant ones.

In mathematical terms, let $\mathcal{F} = \{f_1, f_2, \ldots, f_n\}$ denote the entire collection of features in the dataset, and M represents the ML model. The RFE intends to identify an optimal feature subset $\mathcal{F}^* \subset \mathcal{F}$ that leads to minimal prediction error.

$$\mathcal{F}^* = \arg\min_{F'CF} \mathcal{L}(M(\mathcal{F}')) \tag{4}$$

In the above expression, $\mathcal{M}(\mathcal{F}')$ denotes the model trained on the feature subset $\mathcal{F}'$, and $\mathcal{L}$ signifies the loss function.

3.2.3 LASSO

The LASSO approach enhances the ordinary least squares method by incorporating a regularization term into its objective function. The regularization component is based on the absolute size of the model coefficients. Adjusting the regularization parameter leads to a noticeable reduction of coefficients closer to zero. It can be represented as follows.

$$\min_{\beta_0,\beta}\left(\frac{1}{2n}\sum_{i=1}^{n}(y_i - \beta_0 - \sum_{j=1}^{p}\beta_j x_{ij})^2 + \alpha\sum_{j=1}^{p}|\beta_j|\right) \tag{5}$$

In the above formulation, χ_{ij} represents the independent variable, y_i is the dependent variable, β_j denotes the model coefficients, and the term β_0 refers to the intercept. Furthermore, n points to the number of samples, the term p indicates the number of attributes, and α denotes the regularization parameter.

3.3 PCOS Classification Using FT-Transformer

The FT-Transformer, a simplified Transformer-based model, is utilized to classify PCOS and shows high effectiveness in tabular data analysis [18]. The FT-Transformer is used due to its capability of modeling complex non-linear interactions and feature dependency via a self-attention process, which is tedious to derive via traditional ML classifiers. In addition, the incorporation of FS and optimization algorithms helps to avoid the overfitting problem, which exists in small-sized medical datasets. In the presented model, the clinical data is scaled and fed into the FT-Transformer without tokenization. It also applied feature-wise linear embeddings next to multi-head self-attention blocks for deriving inter-feature dependencies amongst heterogeneous PCOS attributes. In short, this framework converts all features into embeddings and then utilizes stacked Transformer layers to perform classification tasks. In particular, the feature tokenizer method maps the input features x to embeddings $T \in R^{k\times d}$. The representation of feature x_j is obtained through the following embedding computation:

$$T_j = b_j + f_j(x_j) \in R^d \tag{6}$$

where b_j represents the bias associated with jth feature. For various kinds of features (numerical and categorical), the functioning of f_j differs; in short, it could be represented as follows.

$$T = stack[T_1, T_2, \ldots, T_k] \in R^d \tag{7}$$

In the context of the Transformer, the embedding vector of the [CLS] token (classification token) is incorporated into T, and L successive Transformer layers $F_1, F_2, \ldots, F_L$ can be utilized as follows:

$$T_0 = stack\left[[CLS], T\right] \tag{8}$$

$$T_i = F_i(T_{i-1}) \tag{9}$$

To simplify optimization, the PreNorm variant has been utilized effectively. In the PreNorm setup, the first normalization step in the initial Transformer layer must be removed to ensure better results. Figure 2 represents the general diagram of the FT-Transformer. The final embedding of the $[CLS]$ token can be applied for prediction:

$$\hat{y} = Linear(ReLU(LayerNorm(T_L^{[CLS]} \tag{10}$$

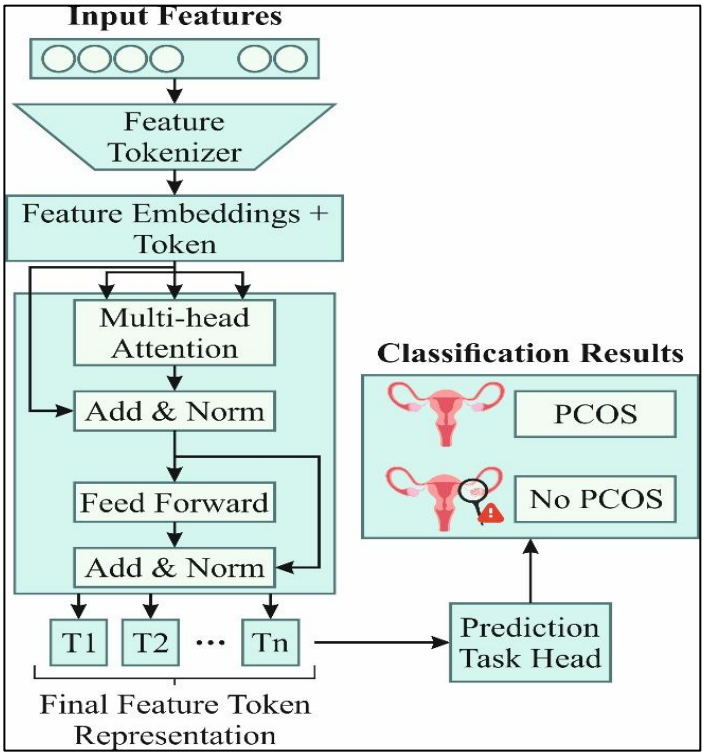

Figure 2. General diagram of FT-Transformer

FT-Transformer is an effective and promising approach to model tabular data, attaining improved efficiency on multiple tasks.

3.4 Model Training and Optimization

To improve stable and reliable training, the network parameters are optimized using the Ranger optimizer [19]. This method integrates RAdam and Lookahead as external and internal optimization algorithms, respectively. The internal optimization algorithm A is responsible for updating the fast weight, and θ is accountable for updating the rules of the fast weight, as outlined below.

$$\theta_{t,i+1} = \theta_{t,i} + A\left(L, \theta_{t,i-1'}, d\right) \tag{11}$$

Here, L indicates the objective function, d signifies a small batch of samples, A refers to the optimizer, $i = 1,2 \ldots k$ indicates the ith batch iteration, and t represents the iteration step.

Slow weight updates depend on the values of the fast weights. When the optimization algorithm A has processed k batches, the update expression for the slow weight ζ is defined as follows.

$$\zeta_{f+1} = \zeta_t + \alpha(\theta_{t,k} - \zeta_t)$$

$$= \alpha[\theta_{t,k} + (1-\alpha)\theta_{t-1,k} + +(1-\alpha)^{t-1}\theta_{0,k}] + (1-\alpha)^t\zeta_0 \quad (12)$$

Table 2 defines the key hyperparameter settings utilized to train the proposed approach, ensuring balanced learning effectiveness and generalized results. A learning rate of 0.001 can be deployed to ensure stable and effective weight updates, while a batch size of 32 permits efficient training with adaptable memory usage. The transformer method is configured with 4 layers, each with an embedding size of 64 and 4 attention heads to capture both local and global attribute dependencies. The feedforward network size is fixed at 128 to improve feature transformation capacity. To check overfitting, a dropout rate of 0.2 and a weight decay of 0.0001 can be used. Furthermore, the Ranger optimizer integrates Lookahead mechanisms, with an alpha value fixed at 0.5 for organized slow weight approximations and k set to 6 to control synchronization frequency, thereby enhancing convergence stability and overall model performance.

Table 2. Parameter setting

Hyperparameter	Description	Parameter Value
Learning Rate	Step size used by the optimizer for updating model weights	0.001
Batch Size	No. of samples processed per training iteration	32
No. of Transformer Layers	Depth of transformer encoder blocks	4
Embedding Dimension	Size of feature token embeddings	64
No. of Attention Heads	No. of heads in multi-head self-attention	4
Feedforward Dimension	Size of the feedforward network in the transformer	128
Dropout Rate	Regularization parameter to avoid overfitting	0.2
Weight Decay	Regularization parameter used in optimization	0.0001
Ranger α (Lookahead)	Slow weight update rate in Ranger optimizer	0.5
Ranger k (Lookahead steps)	No. of fast steps before synchronization	6

3.5 Interpretation with SHAP

Over the past few years, the DL method has seen major improvements, particularly for working with sequential datasets and understanding complex relations. Even though it is highly effective in prediction, DL methods are frequently viewed as black boxes due to their lack of transparency, which hinders wider implementation [20]. SHAP is an approach used to explain predictions made by machine learning models. This can deliver local and global interpretability by breaking down predictions into the individual contributions of each feature. Using the trained methods, the SHAP method is applied to determine SHAP values for the testing data. The mathematical expression for this calculation is shown below:

$$\phi_j = \sum_{S \subseteq N > \{j\}} \frac{|S|!\,(|N| - |S| - 1)!}{|N|!} \big(V(S \cup \{j\}) - V(S)\big) \quad (13)$$

4. Results and Discussion

In this section, the results of the proposed model are discussed. It includes the dataset description, the model's performance, a comparison with other approaches, and explainability results to understand the predictions. The proposed model is simulated using Python 3.6.5 on a PC with an i5-8600k, GeForce 1050Ti 4GB, 16GB RAM, 250GB SSD, and 1TB HDD. The measures used to analyze the results are accuracy, precision, recall, and F1-score.

4.1 Dataset Description

The model is evaluated using the PCOS dataset [21]. PCOS is a condition characterized by uncommon, uneven, or protracted menstrual periods, frequently accompanied by excess androgen levels. Small, fluid-filled cysts accumulate in the ovaries, which can prevent the regular release of eggs. This dataset encompasses all physical and medical parameters to detect PCOS and infertility-related problems. The details of the dataset are given in Table 3. It has a total of 541 instances with two classes; PCOS and No PCOS. Among these, 177 samples belong to the PCOS class, and 364 belong to the No PCOS class. The dataset consists of 44 features, out of which 33 important attributes are chosen after applying a hybrid feature selection process. The final selected features were Age, Weight, Height, BMI, Pulse Rate, Respiratory Rate, Hb, Cycle Length, FSH, LH, Hip Circumference, Waist Circumference, Waist–Hip Ratio, TSH, AMH, PRL, Vitamin D3, Progesterone, RBS, Hair Growth, Skin Darkening, Hair Loss, Pimples, Fast Food Consumption, Regular Exercise, Systolic BP, Diastolic BP, Follicle Number (L/R), Follicle Size (L/R), Endometrium Thickness, and PCOS (Y/N). These features were retained as they showed meaningful relationships and contributed to the prediction of PCOS.

Table 3. Dataset details

Classes	No. of Instances
No PCOS	364
PCOS	177
Total Instances	541

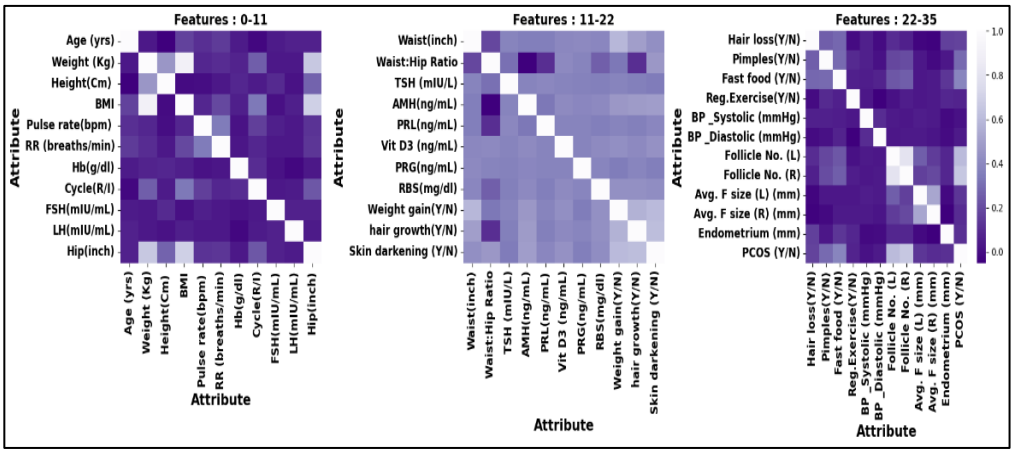

Figure 3. Feature correlation heatmaps across three groups (0–35)

Figure 3 offers correlation heatmaps of features grouped into three subsets, demonstrating the connections among clinical and physiological features. Strong positive connections can be detected along the diagonal in every group, demonstrating attribute self-dependency, but lighter shades highlight adequate inter-feature connections, such as between

BMI, weight, and height. In the second and third groups, certain hormonal and clinical indicators show distinct connections, signifying their relevance in clinical research.

4.2 Detection Performance Results

Table 4 presents the confusion matrices and PCOS classification analysis of the XAIDRL-PCOSD algorithm are presented for 80% and 20% of TRPE/TEPE. The tabulated values indicate that the XAIDRL-PCOSD technique effectively identifies the two samples. From the confusion matrices, the XAIDRL-PCOSD system correctly recognizes and classifies both class labels. Similarly, in the PCOS classification, the XAIDRL-PCOSD methodology correctly distinguishes the two classes, No PCOS and PCOS, under both training and testing splits.

Table 4. Confusion matrices and PCOS classification result of XAIDRL-PCOSD with 80 and 20 splits

Metrics	Training Phase (80%)	Testing Phase (20%)
	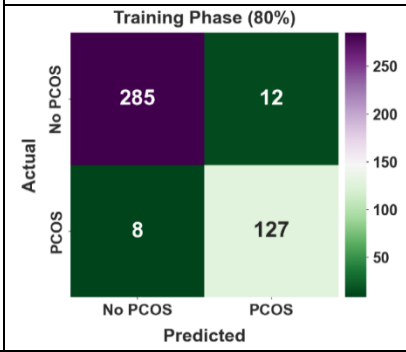	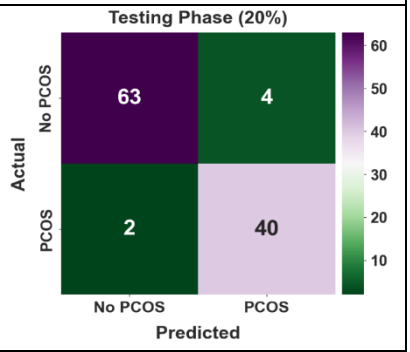
$Accur_y$	95.37	94.50
$Preci_n$	94.32	93.92
$Recal_l$	95.02	94.63
$F1_{Score}$	94.66	94.24
MCC	89.33	88.55

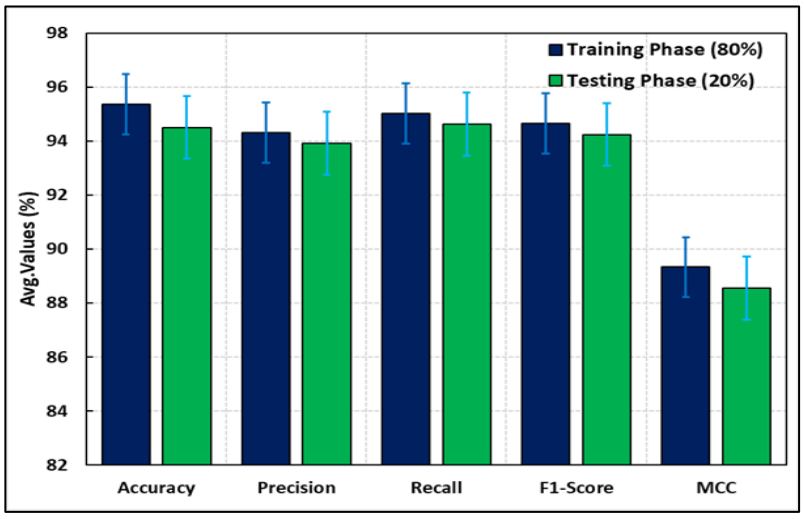

Figure 4. Average of XAIDRL-PCOSD system with 80 and 20 splits

The average PCOS classification outcomes of the XAIDRL-PCOSD system on 80/20 splits are revealed in Figure 4. The outcomes implied that the XAIDRL-PCOSD algorithm can efficaciously classify the samples. With 80%TRPE, the XAIDRL-PCOSD methodology reaches an average $accur_y$ of 95.37%, $preci_n$ of 94.32%, $recal_l$ of 95.02%, $F1_{score}$ of

94.66%, and MCC of 89.33%, correspondingly. Simultaneously, with 20%TEPE, the XAIDRL-PCOSD approach obtained averages $accur_y$ of 94.50%, $preci_n$ of 93.92%, $recal_l$ of 94.63%, $F1_{score}$ of 94.24%, and an MCC of 88.55%, respectively.

Figure 5 displays the training (TRNG) and validation (VLDN) $accur_y$ of the XAIDRL-PCOSD approach with 80/20 splits over 100 epochs. Both curves display a gradual rise $accur_y$ as the epoch counts grow, demonstrating that the model is learning efficiently. Following the epochs, the $accur_y$ curves plateau, proposing that the model has the potential to be a greater solution. Significantly, the TRNG and VLDN curves are thoroughly consistent throughout, signifying little overfitting and optimal generalization on unobserved data.

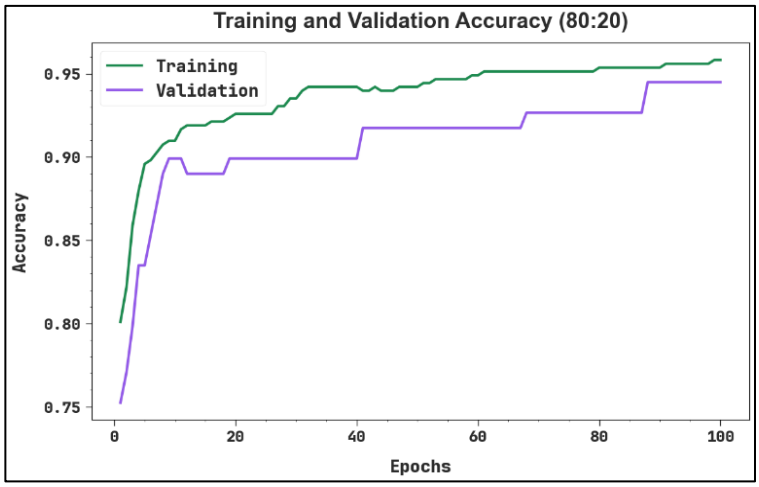

Figure 5. $Accur_y$ curve of the XAIDRL-PCOSD system with 80 and 20 splits

Figure 6 exemplifies the ROC values of the AIDRL-PCOSD with 80/ 20 splits. The figure demonstrates that the proposed model accomplishes enhanced ROC values in both cases. The close correspondence among ROC values specifies greater overfitting and optimum comprehensiveness to hidden information.

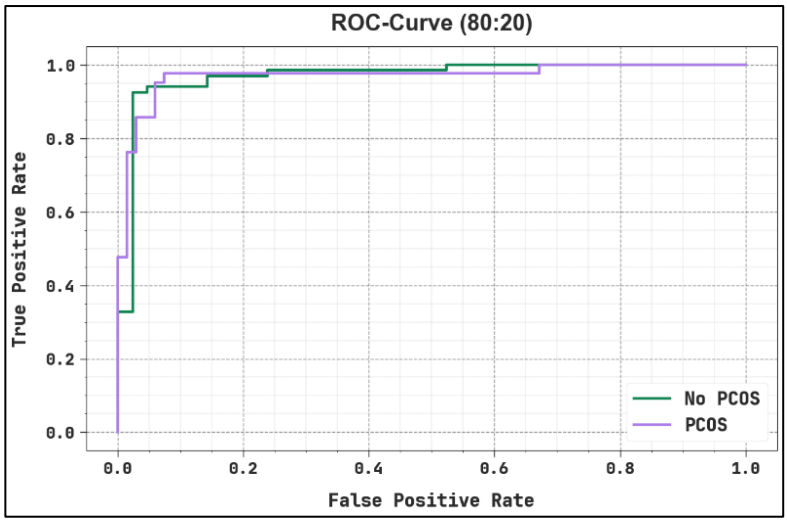

Figure 6. ROC curve of XAIDRL-PCOSD system with 80 and 20 splits

In Table 5, the confusion matrices and PCOS classification analysis of the XAIDRL-PCOSD system are offered for 70% and 30% TRPE/TEPE. The tabulated values show that the XAIDRL-PCOSD approach efficiently distinguishes the two classes. From the confusion

matrices, the XAIDRL-PCOSD system correctly classifies and detects both class labels. Similarly, in the PCOS classification, the XAIDRL-PCOSD method correctly differentiates the two classes, No PCOS and PCOS, under both training and testing splits.

Table 5. Confusion matrices and PCOS classification result of XAIDRL-PCOSD with 70 and 30 splits

Metrics	Training Phase (70%)	Testing Phase (30%)
	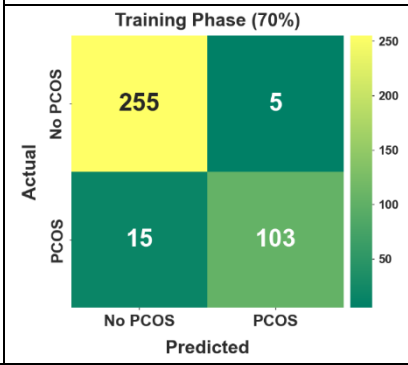	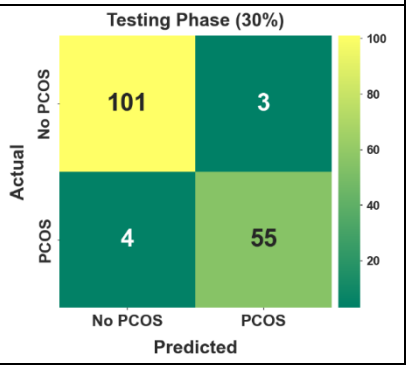
$Accur_y$	94.71	95.71
$Preci_n$	94.91	95.51
$Recal_l$	92.68	95.17
$F1_{Score}$	93.69	95.33
MCC	87.56	90.68

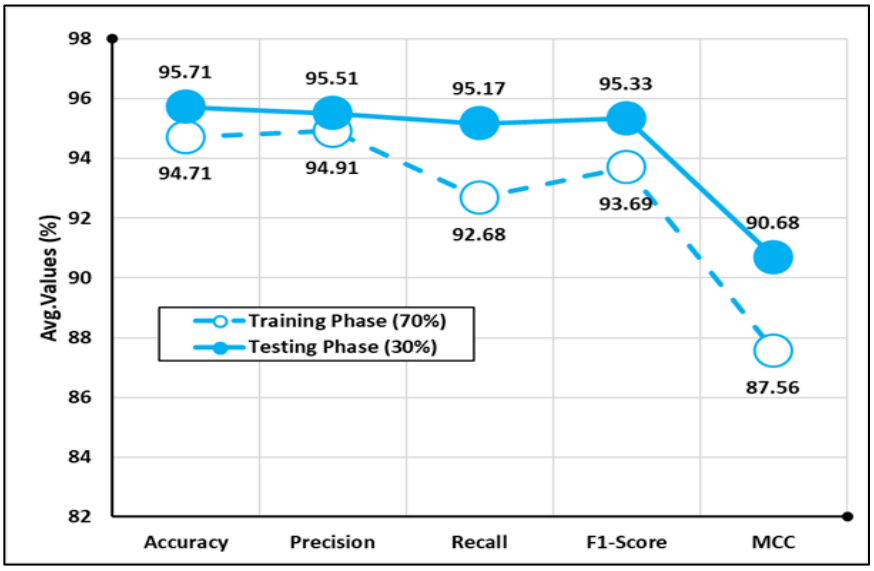

Figure 7. Average of XAIDRL-PCOSD system with 70 and 30 splits

The average PCOS classification outcomes of the XAIDRL-PCOSD approach on 70 and 30 splits are established in Figure 7. The outcomes inferred that the XAIDRL-PCOSD algorithm can efficaciously recognize the two instances. With 70%TRPE, the XAIDRL-PCOSD system obtained an average $accur_y$ of 94.71%, $preci_n$ of 94.91%, $recal_l$ of 92.68%, $F1_{score}$ of 93.69%, and an MCC of 87.56%. Likewise, with 30%TEPE, the XAIDRL-PCOSD technique accomplished averages $accur_y$ of 95.71%, $preci_n$ of 95.51%, $recal_l$ of 95.17%, $F1_{score}$ of 95.33%, and MCC of 90.68%, correspondingly.

Figure 8 depicts the TRNG and VLDN $accur_y$ of the XAIDRL-PCOSD approach with 70 and 30 splits with 100 epochs. Both curves display continued growth $accur_y$ as the count of epoch's develops, demonstrating that the model is learning efficiently. Once around epochs,

the $accur_y$ curves start to plateau, signifying that the model is approaching its best results. Essentially, the TRNG and VLDN curves are thoroughly ranged throughout, resulting in less overfitting and better generalization on unseen data.

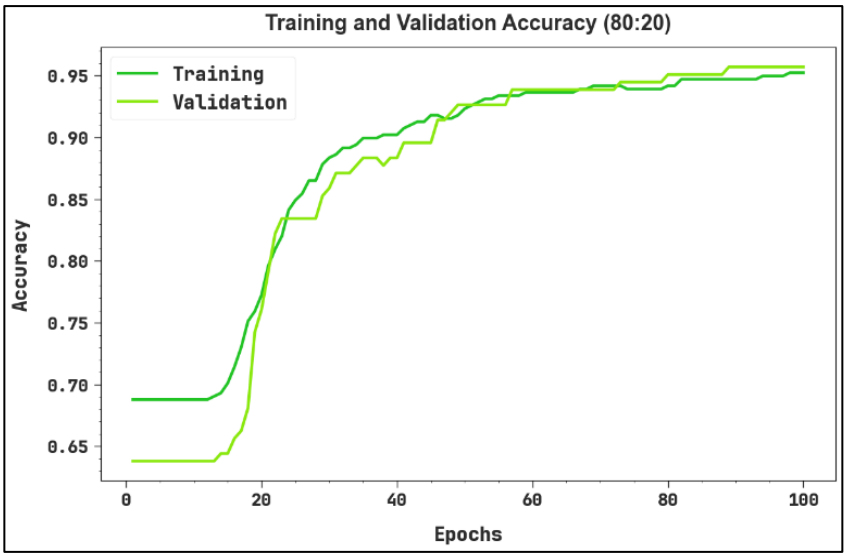

Figure 8. $Accur_y$ curve of the XAIDRL-PCOSD system with 70 and 30 splits

Figure 9 defines the ROC curve analysis of the XAIDRL-PCOSD framework with 70/ 30 splits. The figure exhibits that the proposed model accomplishes enhanced performance under both classes. The increased ROC values of the proposed model under both class labels indicate minimal overfitting and optimal generalization to hidden data.

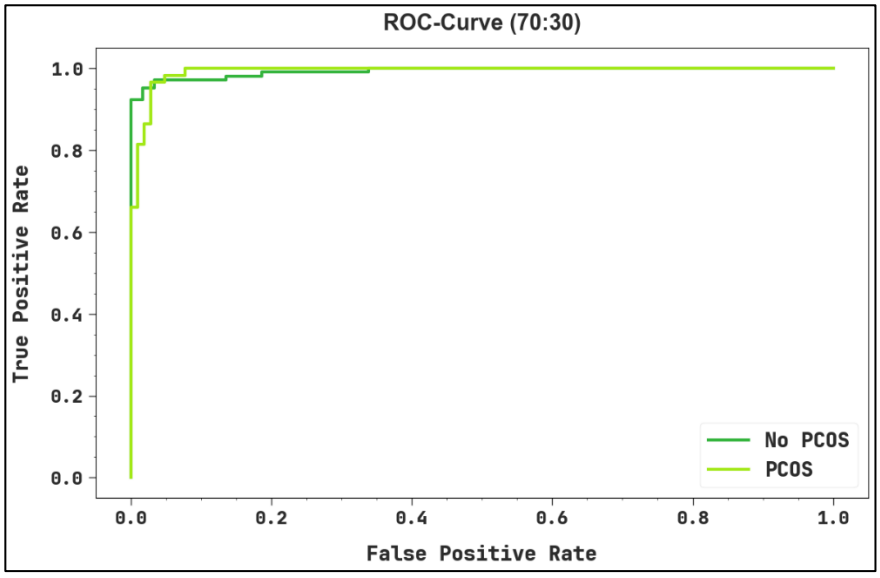

Figure 9. ROC curve of XAIDRL-PCOSD system with 70 and 30 splits

4.3 Comparative Analysis

To establish the efficiency of the proposed XAIDRL-PCOSD methodology, a detailed comparative investigation is presented in Table 6 [22-25]. The simulation results indicate that the Swin Transformer and ConvNeXt techniques depicted poor performance. The MLP, Gradient Boosting, TabTransformer, TabNet, and DenConST models acheived slightly higher performance. Simultaneously, CatBoost, AdaBoost, GIST-MDR+SVM, XGBoost, and WaO

tuned EL algorithms have acquired somewhat greater outcomes. In addition, the hybrid CNN, Logit model+DL, Enhanced FCM, and Custom F-Net methodologies have accomplished moderately closer results. However, the XAIDRL-PCOSD approach outperforms the other approaches with a higher $accur_y$ of 95.71%, $preci_n$ of 95.51%, $recal_l$ of 95.17%, and $F1_{score}$ of 95.33%, respectively.

Table 6. Comparison assessment of the XAIDRL-PCOSD technique with other approaches

Techniques	$Accur_y$	$Preci_n$	$Recal_l$	$F1_{Score}$	Computational Time (sec)
MLP	89.00	87.37	92.56	89.90	8.45
Gradient Boosting	85.00	90.65	86.05	85.47	3.07
TabTransformer	83.80	90.65	91.32	88.44	5.22
CatBoost	90.00	89.33	88.50	90.81	11.00
TabNet	89.45	90.49	87.07	89.25	7.01
AdaBoost	93.05	88.99	86.46	87.71	5.03
Swin Transformer	56.45	60.13	61.57	60.84	9.45
ConvNeXt	58.84	82.62	84.05	83.33	6.11
DenConST	85.69	90.52	91.97	91.24	8.34
Hybrid CNN	95.00	91.76	90.75	90.74	4.93
GIST-MDR+SVM	93.82	90.10	90.76	90.99	2.78
Logit model+DL	94.18	90.88	91.51	91.75	3.43
Enhanced FCM	95.00	90.45	90.69	90.79	4.69
XGBoost	91.00	91.00	92.00	92.00	3.59
Custom F-Net	95.00	91.00	90.00	95.00	4.06
WaO tuned EL	92.80	92.70	92.80	92.70	4.93
XAIDRL-PCOSD	95.71	95.51	95.17	95.33	0.71

The computational time (CTE) analysis of the proposed XAIDRL-PCOSD system is compared with other approaches in Figure 10. The outcomes demonstrated that the XAIDRL-PCOSD algorithm reaches a lower CTE of 0.71s. Conversely, the MLP, Gradient Boosting, TabTransformer, CatBoost, TabNet, AdaBoost, Swin Transformer, ConvNeXt, DenConST, Hybrid CNN, GIST-MDR+SVM, Logit model+DL, Enhanced FCM, XGBoost, Custom F-Net, and WaO tuned EL methodologies reach higher CTE values of 8.45s, 3.07s, 5.22s, 11.00s, 7.01s, 5.03s, 9.45s, 6.11s, 8.34s, 4.93s, 2.78s, 3.43s, 4.69s, 3.59s, 4.06s, and 4.93s, respectively.

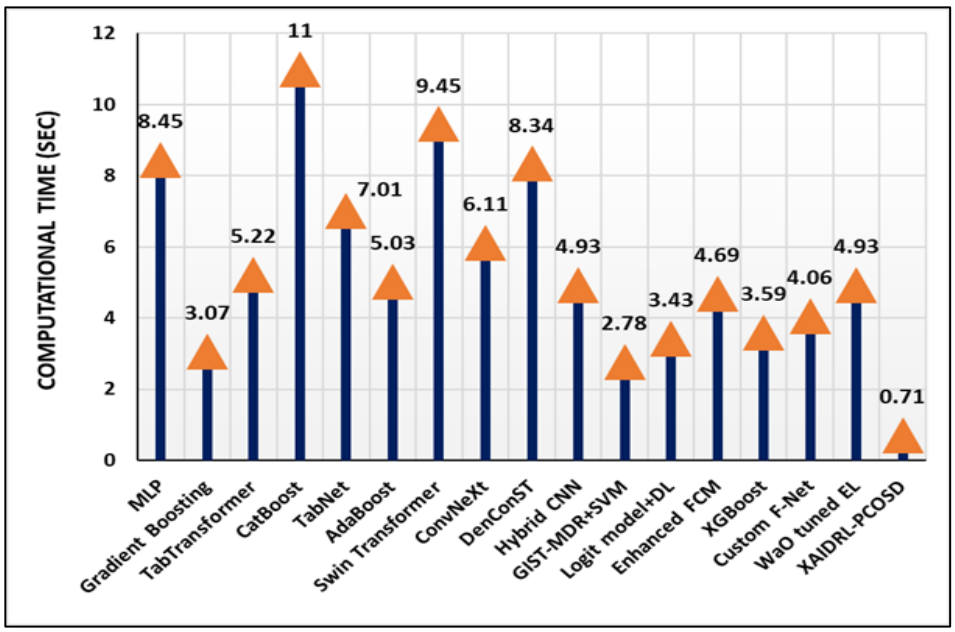

Figure 10. CTE assessment of the XAIDRL-PCOSD approach with other algorithms

The ablation study assesses the contribution of each module in the proposed algorithm by analytically eliminating or modifying it. The outcomes display that every approach significantly enhances overall performance, with a clear drop in accuracy once any important module is excluded. Specifically, the integrated model accomplishes the optimum performance related to individual approaches. This establishes the effectiveness and need of every element in improving model performance. Table 7 represents the ablation study of the XAIDRL-PCOSD approach with various aspects. The Mutual Information (MI FS only) system has portrayed minimal performance of $accur_y$ of 91.71%. In addition, the Recursive Feature Eliminating (RFE FS only) and LASSO Regression for sparsity (LASSO FS only) methodologies have displayed somewhat greater results with $accur_y$ of 92.33% and 93.04%. In the meantime, the Hybrid feature selection process, FT-Transformer only, and FT-Transformer with hybrid feature selection (without Ranger optimizer) methods have demonstrated that reasonable outcomes with $accur_y$ of 93.76%, 94.41%, and 95.01%. Finally, the proposed XAIDRL-PCOSD (FT-Transformer+hybrid feature selection with Ranger optimization process) system has determined the effectual performances with a higher $accur_y$ of 95.71%, $preci_n$ of 95.51%, $recal_l$ of 95.17%, and $F1_{score}$ of 95.33%, correspondingly.

Table 7. Ablation study of the XAIDRL-PCOSD approach with different measures

Techniques	$Accur_y$	$Preci_n$	$Recal_l$	$F1_{Score}$
Mutual Information (MI FS only)	91.71	91.75	91.02	91.37
Recursive Feature Eliminating (RFE FS only)	92.33	92.29	91.81	92.04
LASSO Regression for sparsity (LASSO FS only)	93.04	92.80	92.44	92.78
Hybrid feature selection process	93.76	93.30	93.24	93.35
FT-Transformer only	94.41	93.93	93.94	93.95
FT-Transformer with hybrid feature selection (without Ranger optimizer)	95.01	94.73	94.58	94.73
XAIDRL-PCOSD (FT-Transformer+hybrid feature selection with Ranger optimization process)	95.71	95.51	95.17	95.33

Table 8 represents the K-fold cross-validation of the proposed XAIDRL-PCOSD approach. In Fold-1. $Accur_y$ of 95.31%, $Preci_n$ of 83.26%, $Recal_l$ of 85.53% and $F1_{Score}$ of 91.47%. Additionally, in Fold-2 $Accur_y$ of 91.98%, $Preci_n$ of 83.54%, $Recal_l$ of 92.23% and $F1_{Score}$ of 84.03%. Furthermore, in Fold-3 $Accur_y$ of 88.53%, $Preci_n$ of 88.79%, $Recal_l$ of 91.50% and $F1_{Score}$ of 92.69%. Moreover, in Fold-9 $Accur_y$ of 94.75%, $Preci_n$ of 94.39%, $Recal_l$ of 93.06% and $F1_{Score}$ of 94.32%. Likewise, in Fold-10 $Accur_y$ of 89.47%, $Preci_n$ of 91.20%, $Recal_l$ of 84.14% and $F1_{Score}$ of 91.64%

Table 8. K-fold cross validation of the XAIDRL-PCOSD model

K-Fold Cross Validation	$Accur_y$	$Preci_n$	$Recal_l$	$F1_{Score}$
Fold-1	85.31	83.26	85.53	91.47
Fold-2	91.98	83.54	92.23	84.03
Fold-3	88.53	88.79	91.50	92.69
Fold-4	88.29	89.70	86.98	90.68
Fold-5	84.19	83.35	92.56	92.93
Fold-6	86.32	82.15	90.67	93.53
Fold-7	91.07	88.06	82.83	87.96
Fold-8	83.15	93.36	90.91	91.50
Fold-9	94.75	94.39	93.06	94.32
Fold-10	89.47	91.20	84.14	91.64

4.4 Explainability Results

The SHAP-based interpretability analysis of the model provides insights into integrating global feature importance and local explanations, as shown in Figure 11. Global feature importance identifies highly influential features that affect the entire prediction results and demonstrates that important features impact classifier performance. In contrast, the local SHAP explanation shows how feature values affect a particular prediction's performance.

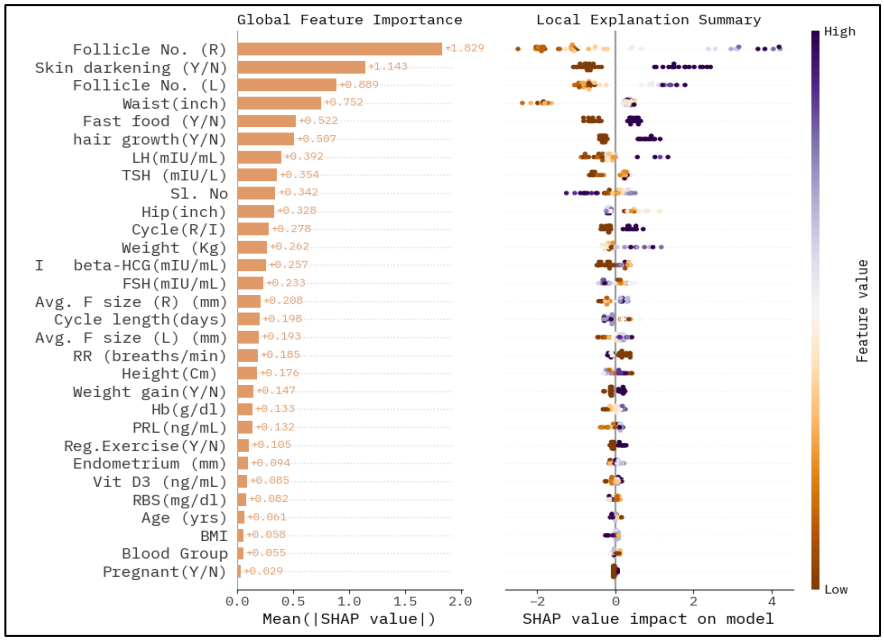

Figure 11. SHAP-based global and local feature importance

The left panel displays that features like follicle count (right and left), skin darkening, and waist size have the maximum total impact on predictions, signifying their strong importance in the model's decision-making. The right panel visualizes how specific feature values affect predictions through samples. Each point signifies a data sample, and its position indicates whether it increases or decreases the prediction. The color gradient reproduces feature intensity, illuminating that greater values of key features (e.g., follicle count and skin darkening) tend to push predictions toward the positive categories, while minimal values contribute less or negatively. These insights improve the transparent nature of the proposed model and enable an effective understanding of its decision-making process. From a clinical perspective, this analysis is useful for identifying clinically related patterns and boosting trust in AI-based decision support systems. The better performance of the proposed XAIDRL-PCOSD system is due to the combination of different components used in this work. The hybrid feature selection method, which integrates MI, RFE, and LASSO, helps in picking the most relevant clinical features while eliminating redundant ones. This reduces redundancy and enhances the overall learning capability of the model. The FT-Transformer model can capture complex dependencies between diverse clinical parameters, which assists in enhancing the prediction of PCOS cases. Moreover, the Ranger optimizer assists in balancing the training process and enhances convergence during model learning. Further, the utilization of SHAP offers a better understanding of how different features contribute to the prediction, which makes the model more transparent. The experimental results, along with the analysis, show that combining feature selection, DL, and explainability assists the model in achieving improved accuracy and reliable performance compared to other approaches.

5. Conclusion and Future Work

This paper presents the XAIDRL-PCOSD model, which supports early and reliable detection of PCOS by employing real-world patient data. The model applies a hybrid feature selection strategy, integrating MI, RFE, and LASSO, to recognize the most important clinical features. For classification, an FT-Transformer is utilized to learn deep feature representations and capture complex relationships among clinical parameters. Moreover, the Ranger optimizer is leveraged to improve convergence and overall model performance. Additionally, XAI is integrated using SHAP to offer clear insights into feature contributions, improving the explainability of the model's predictions for both PCOS and non-PCOS cases. The experimental results exhibit that the proposed technique performs well in detecting PCOS and also provides clear insights into how decisions are made. Because of this, the XAIDRL-PCOSD approach can be used as a useful support tool for medical professionals to understand the important factors involved in diagnosis. Even though the proposed XAIDRL-PCOSD model yields good results for PCOS detection, a few limitations remain. The model is tested only on one dataset, so its performance on other datasets or different populations is not fully clear. While the FT-Transformer model can learn complex relationships, it may require more computational power, which can be challenging in real-time or low-resource settings. Also, model performance can change depending on the selected features and the type of the dataset, so some adjustments may be needed for different clinical cases. Though the proposed model exhibited significant results, a relatively small dataset may affect its generalization abilities under various clinical populations and real-world clinical settings. Therefore, in the future, the proposed method could be validated on large-scale, multi-center, and diverse datasets to ensure reliability and practical applicability. Future work can also focus on designing lighter models that can be used in real-world environments and utilizing real-time clinical data to improve the practical use of the system.

Declarations

Competing Interests and Funding

The authors did not receive support from any organization for the submitted work.

Funding Statement

The authors received no funding for this study.

Human Participants and/or Animals

Not applicable

Ethics Approval

Not Applicable

Conflict of Interest

The authors declare that they have no conflict of interest. The manuscript was written through the contributions of all authors. All authors have given approval to the final version of the manuscript.

Data Availability Statement

The data that support the findings of this study are openly available in Kaggle repository at https://www.kaggle.com/datasets/prasoonkottarathil/polycystic-ovary-syndrome-pcos/data, reference number [21].

Consent to Participate

Not applicable

References

[1] Kurt, Dilara Sarıkaya, Recep Taha Ağaoğlu, Mehmet Ferdi Kıncı, Tuğçe Sırma, Ahmet Kurt, Ramazan Erda Pay, İsmail Burak Gültekin, Hüseyin Levent Keskin, and Sezin Ertürk Aksakal. "Diagnostic Value and Metabolic Association of Serum Clusterin in Women with Polycystic Ovary Syndrome." Diagnostics 16, no. 1 (2026): 167.

[2] Oner, Oznur, Canan Akkus, Doga Demircioglu, Ilhan Karanlik, and Cevdet Duran. "Urinary Albumin-to-Creatinine Ratio Across Phenotypes of Polycystic Ovary Syndrome: A Phenotype-Based Evaluation." (2026).

[3] Prayitno, Gunawan Dwi, Cynthia Retna Sartika, Tono Djuwantono, Andi Wijaya, Raden Muharam, Yudi Mulyana Hidayat, Rima Haifa, Annisah Zahrah, and Keri Lestari. "The Effect of Umbilical Cord-Derived Mesenchymal Stem Cells and Secretome on Metabolomic Profiles (C-Peptide, Adiponectin, Fasting Insulin, and Fasting Glucose): A Randomized Controlled Trial." Journal of Clinical Medicine 15, no. 5 (2026): 1707.

[4] Rahman, Md Ataur, Maroua Jalouli, Mohammed Al-Zharani, and Abdel Halim Harrath. "Next-Generation Dietary Antioxidants in Women's Reproductive Health: Mechanisms, Reproductive Outcomes, And Therapeutic Potential." Antioxidants 15, no. 3 (2026): 319.

[5] Wu, Kaiming, Chang Sun, Ning Din, Jinqian Guo, Jing Li, Zimeng Pan, Ying Wang, Miao Sun, and Hongying Kuang. "AMH Specifically Targets Neuronal AMHR2 to Modulate the Progression of Polycystic Ovary Syndrome." BMC Endocrine Disorders 26, no. 1 (2026): 48.

[6] Parker, Jim, Claire O'Brien, Talat Uppal, and Kelton Tremellen. "Molecular Impact of Metabolic and Endocrine Disturbance on Endometrial Function In Polycystic Ovary Syndrome." International Journal of Molecular Sciences 26, no. 20 (2025): 9926.

[7] Akpang, Nicole, Jakub Kwiatkowski, Lucja Zaborowska, and Artur Ludwin. "Autoantibodies Targeting the Hypothalamic-Pituitary-Ovarian Axis in Polycystic Ovary Syndrome: Emerging Key Players in Pathogenesis?." International Journal of Molecular Sciences 26, no. 9 (2025): 4121.

[8] Maan, Pratibha, Rohit Gautam, Sudharsan Vasudevan, Geetha R. Menon, Amit Arora, Abilash Nair, Puthiyaveettil Khadar Jabbar, and Taruna Arora. "Pharmacological and Non-Pharmacological Interventions for Polycystic Ovary Syndrome (PCOS) In Indian Women: A Systematic Review and Meta-Analysis." Pharmaceuticals 18, no. 5 (2025): 680.

[9] Abed, Baraa Mohammed, Rasha Amer Kadhim, Ihsan Salman, Hussam Shaker Hussein, and Abdullah Farhan Mahdi. "Enhancing Polycystic Ovary Syndrome (PCOS) Diagnosis Using Machine Learning Techniques." INTERNATIONAL JOURNAL OF ADVANCES IN SIGNAL AND IMAGE SCIENCES (2026): 2130-2139.

[10] Suvika, K. V., and D. G. Jyothi. "Early Detection of Polycystic Ovarian Disease Using Optimized Machine Learning Technique." INTERNATIONAL JOURNAL OF ADVANCES IN SIGNAL AND IMAGE SCIENCES (2026): 210-232.

[11] Ahmad, Rumman, Lamees A. Maghrabi, Ishfaq Ahmad Khaja, Louai A. Maghrabi, and Musheer Ahmad. "SMOTE-Based Automated PCOS Prediction Using Lightweight Deep Learning Models." Diagnostics 14, no. 19 (2024): 2225.

[12] Gollapalli, Suneel, P. Kanchanamala, Satish Muppidi, B. Ankitha, Ch Srikanth, and Venubabu Rachapudi. "Enhancing the Detection of PCOS Using DEEP LEARNING." In 2024 2nd International Conference on Self Sustainable Artificial Intelligence Systems (ICSSAS), IEEE, 2024, 736-740.

[13] Jain, Priyanka, Rohit Kumar Mishra, Aakash Deep, and N. K. Jain. "Xplainable AI for Deep Learning Model on PCOD Analysis." In XAI Based Intelligent Systems for Society 5.0, Elsevier, 2024, 131-152.

[14] Avasthi, Vasu, Ashish Kumar, Aditya Bhardwaj, and Tarun Jain. "Empowering Women's Health: Machine Learning for PCOS Detection and Prediction." In 2024 international conference on distributed computing and optimization techniques (ICDCOT), IEEE, 2024, 1-6.

[15] Nalawade, Priyanka, Vishal Borate, Rajlakshmi Narsinha Shindalkar, Snehal Subhash Bansode, Shreya Dilip More, and Cynthia Pachal. "Explainable CNN & Hybrid Deep Learning Model for Health Risk PCOS Prediction & Diagnosis." In 2025 13th International Conference on Intelligent Embedded, MicroElectronics, Communication and Optical Networks (IEMECON), IEEE, 2025, 1-5.

[16] Mondal, Subhash, Anirudh Iyer, and Amitabh Thakur. "An Explainable ANN Framework for Early Detection of PCOS Using SHAP and SMOTETomek." In 2025 Second International Conference on Pioneering Developments in Computer Science & Digital Technologies (IC2SDT), IEEE, 2025, 399-404.

[17] Shakeel, Hafiz Muhammad, Shamaila Iram, Richard Hill, Hafiz Muhammad Athar Farid, Akbar Sheikh-Akbari, and Farrukh Saleem. "A Machine Learning-Based Intelligent Framework for Predicting Energy Efficiency in Next-Generation Residential Buildings." Buildings 15, no. 8 (2025): 1275.

[18] Liu, Jiming, Yi Zhou, Qileng He, and Zhenxing Gao. "ASFT-Transformer: A Fast and Accurate Framework for EEG-Based Pilot Fatigue Recognition." Sensors 25, no. 19 (2025): 6256.

[19] Xie, Fengyun, Linglan Wang, Haiyan Zhu, and Sanmao Xie. "Research on a Rolling Bearing Fault Diagnosis Method Based on Multi-Source Deep Sub-Domain Adaptation." Applied Sciences 13, no. 11 (2023): 6800.

[20] Shen, Zhenzhong, Weigang Han, Yanzhuo Hu, Ye Zhu, and Jingjing Han. "An Interpretable Hybrid Deep Learning Model for Molten Iron Temperature Prediction at the Iron-Steel Interface Based on Bi-LSTM And Transformer." Mathematics 13, no. 6 (2025): 975.

[21] https://www.kaggle.com/datasets/prasoonkottarathil/polycystic-ovary-syndrome-pcos/data.

[22] Ji, Xujiao, Caier Liu, Jing Hu, Sufen Li, Lijun Wang, Xin Cheng, Cong Liu, and Yanjing Zhang. "A Multicenter Deep Learning Framework Integrating Radiomics and Vision Transformers for Comprehensive Ovarian Tumor Analysis from Ultrasound Imaging." European Journal of Medical Research (2026).

[23] Tiwari, Shamik, Amar Shukla, and Akhilesh Kumar Sharma. "Attention-Guided Lightweight Deep Learning Architecture for Classification of Polycystic Ovary Syndrome from Ultrasound Images." Intelligence-Based Medicine (2026): 100358.

[24] Elmannai, Hela, Nora El-Rashidy, Ibrahim Mashal, Manal Abdullah Alohali, Sara Farag, Shaker El-Sappagh, and Hager Saleh. "Polycystic Ovary Syndrome Detection Machine Learning Model Based on Optimized Feature Selection and Explainable Artificial Intelligence." Diagnostics 13, no. 8 (2023): 1506.

[25] Hoque, Md Mahmudul, Md Mehedi Hassain, Muntakimur Rahaman, Md Towhidul Islam, Shaista Rani, and Md Sharif Mollah. "Vision Models for Medical Imaging: A Hybrid Approach for PCOS Detection from Ultrasound Scans." arXiv preprint arXiv:2601.15119 (2026).